HHS Public Access

Author manuscript

J Aerosol Sci. Author manuscript; available in PMC 2024 December 27.

Published in final edited form as:

J Aerosol Sci. 2024 November ; 182: . doi:10.1016/j.jaerosci.2024.106442.

A high-throughput, turbulent-mixing, condensation aerosol concentrator for direct aerosol collection as a liquid suspension

Orthodoxia Zervaki[a,b], **Dionysios D. Dionysiou**[b,1], **Pramod Kulkarni**[a,*]

[a]National Institute for Occupational Safety and Health, Centers for Disease Control and Prevention, Cincinnati, OH, 45226, United States

[b]Environmental Engineering and Science Program, Department of Chemical and Environmental Engineering (ChEE), University of Cincinnati, Cincinnati, OH, 45221, United States

Abstract

Trace measurement of aerosol chemical composition in workplace atmospheres requires the development of high-throughput aerosol collectors that are compact, hand-portable, and can be operated using personal pumps. We describe the design and characterization of a compact, high flow, Turbulent-mixing Condensation Aerosol-in-Liquid Concentrator (TCALC) that allows direct collection of aerosols as liquid suspensions, for off-line chemical, biological, or microscopy analysis. The TCALC unit, measuring approximately 12 × 16 × 18 cm, operates at an aerosol sample flowrate of up to 10 L min^{-1}, using rapid mixing of a hot flow saturated with water vapor and a cold aerosol sample flow, thereby promoting condensational growth of aerosol particles. We investigated the effect of operating parameters such as vapor temperature, growth tube wall temperature, and aerosol sample flowrate, along with the effect of particle diameter, inlet humidity, aerosol concentration, and operation time on TCALC performance. Nanoparticles with an initial aerodynamic diameter ≥25 nm could grow to droplet diameters >1400 nm with an efficiency ≥80%. Good droplet growth efficiency was achieved for sampled aerosol relative humidity ≥9%. We measured complete aerosol collection for concentrations of ≤3 × 10^5 cm^{-3}. The results showed good agreement between the particulate mass collected through the liquid collector and direct filter collection. The TCALC eliminates the need for sample preparation and filter digestion during chemical analysis, thereby increasing sample recovery and substantially improving the limit of detection and sensitivity of off-line trace analysis of collected liquid samples.

*Corresponding author.: PSKulkarni@cdc.gov (P. Kulkarni).

[1]Deceased.

Declaration of competing interest

The authors declare that they have no known competing financial interests or personal relationships that could have appeared to influence the work reported in this paper.

Appendix A. Supplementary data

Supplementary data to this article can be found online at https://doi.org/10.1016/j.jaerosci.2024.106442.

CRediT authorship contribution statement

Orthodoxia Zervaki: Writing – original draft, Methodology, Investigation, Formal analysis, Data curation, Conceptualization. **Dionysios D. Dionysiou:** Supervision. **Pramod Kulkarni:** Writing – review & editing, Supervision, Resources, Project administration, Funding acquisition, Conceptualization.

Disclaimer: The findings and conclusions in this report are those of the author(s) and do not necessarily represent the official position of the National Institute for Occupational Safety and Health, Centers for Disease Control and Prevention.

Handling Editor: Chris Hogan

Keywords

High flowrate; Aerosol collection; Liquid suspension; Condensational growth; Supersaturation; Rapid mixing

1. Introduction

Filter collection is the most common air sampling method when monitoring air quality in workplace atmospheres. For chemical analysis of the collected particulate filter sample, offline laboratory analytical methods are often used, which require time-consuming and labor-intensive sample preparation and pretreatment methods. Additionally, filters are susceptible to the adsorption and/or evaporation of moisture and/or volatile organic compounds contributing to increased measurement uncertainty (Barhate et al., 2022; Liu et al., 2014). Sample extraction from filters or other collection substrates or sample resuspension is often required for various analytical methods, such as for crystalline silica quantification using X-Ray Diffraction (XRD) in NIOSH Method 7500 (NIOSH, 2003a) or for the detection of metals using Inductively Coupled Plasma, Atomic Emission Spectroscopy (ICP-AES) in NIOSH Method 7300 (NIOSH, 2003b). However, these invasive sample preparation methods may result in sample damage or analyte loss (Daher et al., 2011; Gao et al., 2017), leading to poor detection limits or measurement uncertainty.

The condensation droplet growth technique has been widely employed for real-time aerosol measurement (Agarwal & Sem, 1980; Bricard et al., 1976; Cheng, 2011; Hering et al., 2019; Hering et al., 2005; Ryan et al., 2015; Sinclair & S.Hoopes, 1975). Condensation droplet growth apparatuses have also been effectively combined with inertial impaction for dry spot sample collection and offline chemical analysis (Eiguren Fernandez et al., 2014; Zervaki et al., 2024; Zervaki et al., 2023). However, impaction inherently limits sampling flowrates because the heating of the collection substrate must be sufficient for rapid water evaporation to achieve dry sample collection. The droplet growth technique through condensation at high flowrates has been effectively integrated with direct collection in aqueous suspensions for bioaerosol collection (Jang et al., 2022; Nannu Shankar et al., 2024) and inorganic aerosol collection (Khlystov, 1995; Kidwell & Ondov, 2001; Orsini et al., 2003; Sorooshian et al., 2006; Wang et al., 2013; Weber et al., 2001). However, these systems often involve cumbersome devices that are impractical for occupational or field applications requiring portability and automated operations.

Here we describe the development of a compact, high-throughput, Turbulent-mixing Condensation Aerosol-in-Liquid Concentrator (TCALC) designed for the direct collection of aerosols as a liquid suspension. The turbulent mixing condensational technique offers several advantages: it allows high sampling flowrates, reduces diffusional losses (Kim et al., 2002; Mavliev, 2002) enables fast droplet growth (Cheng, 2011; Wang et al., 2002) and results in more compact instrument geometries (Zervaki et al., 2024). The TCALC system utilizes an aerosol sampling flowrate of up to 10 L min^{-1}. We investigated instrument performance as a function of operating parameters such as: (i) the temperature of the vapor, (ii) the temperature of the growth tube wall, (iii) aerosol diameter, (iv) inlet relative

humidity, and (v) aerosol number concentration. We also compared the collection efficiency of the TCALC with that of the particulate filter collection.

2. Materials and methods

2.1. Description of the TCALC

We have recently developed and evaluated a compact, high-flow, Turbulent-mixing Condensation Aerosol Concentrator (TCAC), designed for the direct collection of particles as a dried spot sample for analysis using various laser spectroscopy and microscopy methods (Zervaki et al., 2024). The TCALC described in this work further builds on TCAC design to address specific needs with respect to high aerosol sample flow throughput and direct aerosol concentration into a liquid. The scheme involves rapid mixing of a cold, aerosol flow with a hot, water-vapor saturated flow, promoting condensational droplet growth to diameters that are easily collected via impaction. The TCAC scheme was modified to accommodate much higher aerosol sampling flowrates and enable direct aerosol collection as a liquid suspension. The modified device, referred to as the “TCALC”, is shown in Fig. 1. It measures approximately 12 × 16 × 18 cm, and weighs less than 2 lb.

The hot water vapor flow is generated in the *saturator*, as described elsewhere (Zervaki et al., 2024). A particle-free air flow with a flowrate in the range of 1–2.5 L min^{-1} is introduced into a 30-cm-long, 2-mm-ID Nafion™ membrane tube (TT-110; Perma Pure LLC, Lakewood NJ), which is immersed in heated, distilled ultra-filtered water. The Nafion™ tube, a proton-exchange membrane, enables water vapor saturation of the particle-free airflow. A temperature controller (CN4116-R1-R2-LV; Omega, Norwalk CT) regulated the water temperature at 70, 75, 80 or 85 °C, using a cartridge heater (Yancheng Xinrong Electronics Industry, Ltd., China) and a resistance temperature detector (RTD-NPT-72-E; Omega Engineering Inc, Norwalk CT).

The hot, vapor-saturated flow exits the saturator through a 35-mm-long, clear polyvinyl chloride 0.0625” ID tubing and enters the *mixing region* through a 4-mm ID inlet, with a flow velocity ranging from 1.3 to 3.3 m s^{-1}. Simultaneously, the aerosol flow is introduced from the top of the mixing region, to eliminate potential wall losses, at an ambient temperature of 22 °C, through a 10-mm ID inlet, with a flowrate ranging from 8 to 10 L min^{-1}. The hot, vapor-saturated flow mixes rapidly at a 90-degree-angle with the cold aerosol flow, generating supersaturation and thereby promoting condensational growth of particle-encapsulated droplets(Sgro and Fernández de la Mora, 2004; Kim et al., 2003; Kousaka et al., 1982; Okuyama et al., 1984; Parsons and Mavliev, 2001; Wang et al., 2002).

The mixed flow is then introduced into the *droplet growth region*, which comprises of a 23-mm ID and 64-mm long aluminum cylinder with flat external surfaces. The growth tube is cooled using a set of thermoelectric coolers (CP14-127-045-L1-W4.5, Laird Thermal Systems, Morrisville NC). The two thermoelectric coolers along with a thermistor (TCS610; Wavelength Electronics, Bozeman MT) are connected to a temperature controller (MPT10000; Wavelength Electronics, Bozeman MT) to maintain desired temperature of the growth tube wall (in the range of 0–15 °C). In the growth tube region, the mixing of the cold aerosol flow with the hot vapor-saturated flow continues, further extending supersaturation,

nuclei activation, and droplet growth. This process is enhanced by cooling the growth tube walls (Parsons & Mavliev, 2001; Weber et al., 2001). The internal cylindrical surface of the growth tube is covered with a rolled Durapore® PVDF membrane filter (GVWP00010; Sigma Aldrich Inc., St. Louis MO), where excess water vapor is condensed. The condensed water on the growth tube wall is then removed using a peristaltic pump. Separation of the aerosol sample from the condensed vapor from the walls enhances analytical detection limits (Wang et al., 2020; Wubulihairen et al., 2015).

Downstream of the droplet growth region, the grown droplets are directed into a narrow beam via a *focusing nozzle*. The jet diameter of the nozzle (D_j) was calculated as follows (Hinds and Zhu, 2022):

$$D_j = \frac{\rho_p d_{p50}^2 U C_c}{9 \mu Stk_{50}} \quad (1)$$

where ρ_p is the particle density, d_{p50} is the particle diameter corresponding to 50% collection efficiency, U is the jet velocity, C_c is the Cunningham slip correction factor, μ is the air dynamic viscosity, and Stk_{50} is the Stokes number corresponding to 50% collection efficiency. For a round jet nozzle, Stk_{50} is typically equal to 0.24. We determined that a nozzle diameter (D_j) of 2.5 mm would effectively capture droplets with $d_p \geq 1.7$ μm or $d_p \geq 1.4$ μm, at flowrates of 9 L min^{-1} or 12.5 L min^{-1}, respectively (Hinds and Zhu, 2022). These flowrates represent the minimum and maximum flowrates used, including both the aerosol and vapor streams.

After exiting the focusing nozzle, the grown droplets impinge on the internal wall surface of a second converging nozzle, which serves as the *droplet impactor*. The droplet impactor was designed to allow droplets to slide towards a 1.5-mm ID hole and accumulate in a small, easily replaceable polypropylene vial, forming a liquid suspension.

2.2. Experimental setup

2.2.1. Droplet growth efficiency—We measured the droplet growth efficiency, which refers to the initiation of vapor condensation on the surface of the aerosol particles acting as nuclei and the growth, achieved through the TCALC as a function of the temperature of the vapor flow generated through the saturator (T_{sat}), the temperature of the growth tube wall (T_{gt}), the aerodynamic diameter of the seed particles (d_p) and the relative humidity of the aerosol stream (RH). The experimental set up used is shown in Fig. 2.

Sodium chloride aerosol was generated through a jet nebulizer (Salter 8900 Series; Salter Labs, Arvin CA), and was subsequently dried using a diffusion dryer (model 3062, TSI Inc., Shoreview MN), containing silica gel desiccant. Near-monodisperse aerosol of desired aerodynamic diameter (d_p = 25, 50, 75, 100, 150, 200, 250 and 300 nm), was obtained using an Aerodynamic Aerosol Classifier (AAC; Cambustion Ltd, Cambridge, United Kingdom) operating at 1.5 L min^{-1}.

Upstream of the mixing region of the TCALC, two humidifiers (MH-110-12F-4; Perma Pure LLC, Lakewood NJ) were placed: one was placed downstream of the AAC and the second was placed in parallel with a valve, controlling the relative humidity of the dilution air and subsequently of the aerosol flow. The aerosol flow was introduced in the mixing region at a flowrate (Q_a) of 8, 9 or 10 L min^{-1}, an ambient temperature (T_a) of 22 °C, and an RH in the range of 9–60%.

Water vapor was generated through the saturator at a fixed temperature of 70, 75, 80 and 85 °C. For these saturator temperatures, we have calculated the saturation ratio (S_R) and Kelvin diameter (seed particle diameter that neither grows nor evaporates; d_p*) as a function of the ratio of vapor-to-aerosol flowrate (see Section S1 in the SI). Figure S-1 in the SI shows that different saturator temperatures required different vapor-to-aerosol flowrate ratios (Q_v/Q_a), to reach maximum S_R or minimum d_p*. Therefore, when the aerosol flow temperature (T_a) is 20 °C, a vapor-to-aerosol flowrate ratio of 0.25, 0.23, 0.18 and 0.13 should be used for a T_{sat} of 70, 75, 80, and 85 °C, to achieve S_R of approximately 1.9, 2.1, 2.3 and 2.5, respectively (Zervaki et al., 2024). Particle-free air was introduced into the saturator, and a vapor-saturated flow was produced at a controlled flowrate (Q_v) of 1, 1.2, 1.3, 1.4, 1.6, 1.8, 2, 2.3 or 2.5 L min^{-1}.

Following the mixing of the cold aerosol flow with the hot vapor-saturated flow, the mixed flow was introduced into the droplet growth region, which was further “actively” cooled using thermoelectric coolers. The temperature of the growth tube was controlled at 0, 5, 10, and 15 °C. We also evaluated the collector when no cooling was applied on the droplet growth region.

A Condensation Particle Counter (model UWCPC 3786; TSI Inc., Shoreview MN) was used along with an Optical Particle Sizer (model OPS 3330; TSI Inc., Shoreview MN) downstream of the droplet growth region to assess the droplet growth efficiency. The CPC measured the number concentration of particles with a diameter of 2.5 nm–3 μm, and the OPS measured the number concentration of particles within a diameter in the range of 300 nm to 10 μm. Measuring droplet size distribution and growth efficiency right at the exit of the condensational growth apparatus is impractical when using particle counters. To address this, the tubing used to transport the droplet stream from the droplet growth region to the particle counters was shielded with fiberglass woven tape to maintain the temperature of the droplet flow, preventing changes in droplet size distribution. Additionally, sharp bends and elbows were avoided to reduce wall losses and the tube length from the droplet growth region to the counters was identical to ensure similar inertial droplet losses for both particle counters. Measured growth efficiencies would serve as conservative estimates in case of appreciable droplet wall loss. Along with the CPC and the OPS, an external vacuum pump was used downstream of the TCALC to control the inlet aerosol flowrate at 8, 9 or 10 L min^{-1}.

Within the TCALC, the collection of enlarged droplets relies on inertial impaction. Thus, droplet growth to $d_p > 1.4$ μm is imperative. It is worth noting that optical particle counters often underestimate the size of water droplets (Hinds & Kraske, 1986), and their true

aerodynamic diameter is expected to be larger than their measured optical diameter (d_d). In this study, the measured droplet growth efficiency refers to particle activation and droplet growth to $d_d > 1.4$ μm. That corresponds to an estimated aerodynamic diameter ≥1.8 μm ()(Chien et al., 2016; Zervaki et al., 2024), sufficiently large for inertial collection. The droplet growth efficiency (η) was calculated as follows:

$$\eta = \frac{N_{OPS}}{N_{CPC}} \tag{2}$$

where N_{OPS} denotes the number concentration with $d_d > 1.4$ μm, as measured by the OPS, and N_{CPC} denotes the total number concentration as measured by the CPC.

2.2.2. Number concentration effect—The performance of the TCALC was also evaluated as a function of the particle number concentration of the inlet aerosol flow (Figure S-2 in the SI). Crystalline silica test aerosol was generated using a fluidized bed aerosol generator (model 3400A, TSI Inc., Shoreview MN). The generator used a fine, ground silica powder (Min-U-Sil@5; US Silica, Katy TX) as the source material. The size distribution of the generated silica particles at the outlet of the fluidized bed is shown in Figure S-3 in the SI. To control the number concentration of the aerosol, the generated aerosol flow was diluted with particle-free air downstream of the fluidized bed. The aerosol flowrate at the inlet of the collector was fixed at 10 L min^{-1}, and the relative humidity (RH) and temperature of the aerosol stream (T_a) were approximately 41.5% and 22.5 °C, respectively. The temperature of the generated vapor (T_{sat}) and the growth tube wall (T_{gt}) was controlled at 85 °C and 0 °C, respectively.

A butanol-based Condensation Particle Counter (model CPC 3776, TSI Inc., Shoreview MN) was used downstream of the collector to quantify the fraction of the particles that were not captured by the TCALC. The CPC was also used upstream of the TCALC to measure the particle concentration at its inlet. The collection efficiency ($C.E.$) achieved through the TCALC was calculated as follows:

$$C.E. = \frac{N_i - N_o}{N_i} \tag{3}$$

where N_i is the number concentration of the aerosols measured at the inlet of the collector, and N_o is the number concentration of the aerosols that were not collected in the TCALC.

2.2.3. Comparison with direct filter collection—The collection efficiency of the TCALC was compared to that of the filter-based collection method. We used the experimental setup shown in Figure S-4 in the SI. Crystalline silica was generated using a fluidized bed aerosol generator. The size distribution of the generated aerosol at the outlet of the fluidized bed is shown in Figure S-3 in the SI. The relative humidity (RH) of the

aerosol stream ranged from 42.2% to 74.8%. The average temperature of the aerosol stream (T_a) was approximately 21.5 °C.

The crystalline silica was collected simultaneously by the TCALC at a flowrate of 10 L min^{-1}, and a reference 0.4-μm pore size, 37-mm polycarbonate filter (225–1609; SKC Inc., Eighty Four PA) at a flowrate of 10 L min^{-1}. The filter was placed in a closed-face filter cassette, collocated, and operated in parallel with the TCALC. A DustTrak™ DRX (model 8533, TSI Inc., Shoreview MN) was used in parallel with the TCALC and the filter cassette to monitor the mass concentration collected. When the collected particulate mass on the filter was estimated to have exceeded 100 μg, the reference filter was replaced during the collection process, to prevent sample "overloading" on the filter and a potential increase of the pressure drop (Raynor et al., 2011). The total mass collected on all the reference filters for each measurement was calculated by summing the individual filter gravimetric measurements.

Following the collection, both the droplet impactor and the collection vial of TCALC were removed to recover the collected crystalline silica particles. The droplet impactor was rinsed with 3 ml of isopropyl alcohol, allowing for the retrieval of trace particles adhering to the droplet impactor surface. The liquid rinse containing particles was combined with the collected suspension. The suspension was then vacuum-filtered through a 20 μm or 30 μm-pore-sized mesh nylon filter, with a diameter of 25 mm (NY2002500, NY3002500; Millipore Sigma, St. Louis MO) and a 0.4-μm pore size, 25-mm-diameter polycarbonate filter (225–1608; SKC Inc., Eighty Four PA). The mesh nylon filter ensured removal of any impurities collected, including traces from the conductive silicone rubber tubing used for the sampling. The polycarbonate filter was used to recover the silica particles. The collection vial was rinsed with an additional 3 ml of isopropyl alcohol and the rinse was also subjected to filtration. The 25-mm-diameter polycarbonate filter was then placed in a temperature and relative humidity-controlled environment along with the 37-mm-diameter reference filter used during the aerosol collection, to dry. A microbalance (XPR6U Microbalance; Mettler Toledo, Columbus OH) was used for weighing the filters. The analyte mass collected on the filters (m_p) was then calculated:

$$m_p = M_f - M_i \tag{4}$$

where M_f and M_i denote the final and initial filter mass, respectively.

3. Results and discussion

3.1. Saturator temperature effect

Fig. 3 shows the effect of the temperature of the saturator (T_{sat}) on the droplet growth efficiency of the TCALC. Higher sampling flowrates required higher saturator temperatures to achieve near–complete activation. Particularly, when the aerosol flowrate was fixed at 8 L min^{-1}, droplet growth efficiency remained ≥89% at $T_{sat} \geq 75$ °C. When the aerosol flowrate

was 9 L min^{-1}, droplet growth efficiency exceeded 92% at $T_{sat} \geq 80$ °C. Similarly, at an aerosol flowrate of 10 L min^{-1}, droplet growth efficiency was >90% at $T_{sat} = 85$ °C.

The highest droplet growth efficiency was consistently observed for $T_{sat} = 85$ °C across all tested aerosol flowrates. This was attributed to the greater temperature differential (ΔT) between the hot vapor and cold aerosol flow, which induces higher saturation ratios (Okuyama et al., 1984, 1987). However, droplet growth could not be achieved at any of the tested flowrates when $T_{sat} = 70$ °C. Droplet growth efficiency to $d_d > 300$ nm, $d_d > 700$ nm, and $d_d > 1400$ nm for the different aerosol flowrates at different T_{sat} was measured (Figure S-5 in the SI). These data suggest that the lower efficiencies shown in Fig. 3 are more likely due to insufficient nuclei activation rather than insufficient growth of the droplets. This effect indicates a potential reduction in saturation ratio, perhaps due to a lower-than-expected temperature differential (ΔT) between the hot vapor-saturated and cold aerosol flow in the TCALC. Subsequently, a T_{sat} of 75, 80 and 85 °C can be used for an aerosol flowrate of 8, 9 and 10 L min^{-1}, respectively.

The greatest ΔT employed here corresponded to approximately 60 °C. Turbulent-mixing condensational droplet growth collectors usually employ higher ΔT (Okuyama et al., 1984; Parsons & Mavliev, 2001; Weber et al., 2001) compared to the laminar-based condensational droplet growth collectors, where the ΔT is typically around 30–35 °C (Eiguren Fernandez et al., 2014; Zervaki et al., 2023). However, the turbulent mixing condensational technique allows significantly higher flowrates in more compact instrument sizes (Zervaki et al., 2024).

3.2. Particle diameter and operation time effect

Fig. 4 (a) shows the effect of seed particle aerodynamic diameter on the performance of the TCALC. We measured consistent droplet growth efficiencies for all tested aerosol flowrates. Droplet growth efficiency was ≥80% for $d_p \leq 75$ nm, and consistently surpassed 90% for seed particles with $d_p \geq 100$ nm across all tested flowrates. This shows that the TCALC can be effectively used for collection of particles in the diameter range tested ($d_p \geq 25$ nm).

We further examined the impact of the operation time of the TCALC on the droplet growth efficiency ($d_d > 1.4$ μm) (Fig. 4 (b)). The collector consistently exhibited reliable performance throughout an uninterrupted 60-min operation while activating sodium chloride aerosol with a seed aerodynamic diameter of 100 nm. At an aerosol flowrate of 8 L min^{-1} ($T_{sat} = 75$ °C), a droplet growth efficiency of ≥78% was observed. At aerosol flowrates of 9 L min^{-1} ($T_{sat} = 80$ °C) and 10 L min^{-1} ($T_{sat} = 85$ °C), a more stable droplet growth efficiency was observed (≥86%) as a function of time. The reason for the somewhat unstable growth efficiency at 8 L min^{-1} is unclear and could likely be attributed to lower saturation ratio and an increasing uncertainty in measured growth efficiency at 8 L min^{-1}. It is worth noting that a higher ΔT is expected to yield near-complete activation of seed particles. Based on this data, we expect that the design of the mixing chamber in TCALC is adequate to prevent heat transfer between hot and cold flows (just before turbulent mixing) over few hours.

3.3. Growth tube temperature effect

Fig. 5 shows the effect of the growth tube temperature (T_{gt}) on the droplet growth efficiency of TCALC. We measured the highest efficiency (≥89%) at $T_{gt} = 0$ °C across all tested aerosol flowrates. This indicates that acceptable operation performance of the TCALC necessitates cooling of the droplet growth region. However, the effect of the growth tube temperature was greater at lower aerosol flowrates ($Q_a = 8$ L min^{-1} or $Q_a = 9$ L min^{-1}) compared to higher aerosol flowrates $\left(Q_a = 10 \text{ L min}^{-1}\right)$. The saturator temperature set for each aerosol flowrate varied– $T_{sat} = 75$ °C at 8 L min^{-1}, $T_{sat} = 80$ °C at 9 L min^{-1}, and $T_{sat} = 85$ °C at 10 L min^{-1}.

The efficiency of seed particle activation and droplet growth is directly related to the level of saturation achieved at the mixing point of the cold aerosol flow with the hot vapor-saturated flow. This saturation ratio is influenced by the temperature differential between the two flows and the ratio of vapor-to-aerosol flowrate, irrespective of their individual magnitudes. However, mixing of the two flows is not limited in the mixing region but can be also extended in the droplet growth region, leading to further particle activation and droplet growth. Therefore, high activation and droplet growth efficiency was anticipated when the highest saturator temperature was used ($T_{sat} = 85$ °C) and/or at increased residence times within the droplet growth region. However, further experiments are necessary to investigate whether the saturation ratio at the mixing region or the residence time of the particles/droplets in the droplet growth region has a greater impact. These experiments would involve measuring droplet growth efficiency for different saturator temperatures set at a fixed aerosol flowrate, or varying aerosol flowrates at a fixed saturator temperature.

3.4. Relative humidity effect

Fig. 6 shows the droplet growth efficiency measured as a function of the relative humidity of the input aerosol flow. A T_{sat} of 85 °C was used at all aerosol flowrates. At an aerosol flowrate of 8 L min^{-1}, the droplet growth efficiency was >90% for $RH \geq 20\%$ and it remained >80% at an RH of 9%. At a flowrate of 9 L min^{-1}, we measured a droplet growth efficiency of ≥80% down to 30%RH, dropping below 50% at an RH of ≤20%. At an aerosol flowrate of 10 L min^{-1}, the droplet growth efficiency measured was >85% at RH values of ≥40%, but decreased significantly at lower RH.

Higher supersaturation ratios can be reached by increasing the water vapor content or relative humidity of the aerosol flow, thereby enhancing seed activation and droplet growth. Lower inlet aerosol flowrates resulted in higher droplet growth efficiencies even at low humidity levels of the input aerosol flow. This was attributed to the prolonged residence time of the mixed flow within the TCALC when lower aerosol flowrates were used.

3.5. Number concentration effect

Fig. 7 shows the measured collection efficiency of polydisperse silica particles relative to the particle number concentration. The collection efficiency remained consistently high (>95%) up to a particle number concentration of 3×10^5 cm^{-3}, beyond which it decreased to 56% at a particle number concentration of 10^6 cm^{-3}.

The observed drop in collection efficiency at higher particle number concentrations has been investigated before for various condensation droplet growth collectors, as discussed by Lewis and Hering (2013). Water-based, laminar-flow condensation particle counters and collectors often suffer from heat release from water vapor condensation on particles, leading to elevated temperatures and subsequent reduction in the saturation ratio. Our previous study (Zervaki et al., 2024) showed the effect of increased number concentration on the activation and growth efficiency of 25-nm-diameter sodium chloride particles using "TCAC" for spot sample collection, which became prominent at a number concentration of $\geq 3 \times 10^4$ cm^{-3}. In the current study, we evaluated the effect of number concentration on a polydisperse silica test aerosol. We did not probe the minimum nuclei diameter that can be collected at high number concentrations; however, our results suggest that collection is highly efficient when particulate mass is used as a performance metric.

3.6. Comparison with direct filter collection

Fig. 8 shows a comparison between crystalline silica mass collected through the TCALC and through direct filter collection. Good agreement is observed between the two aerosol collection techniques. A linear fit curve was plotted to the experimental data, with a slope of 0.98 and high linearity $\left(R^2 = 1\right)$.

Minor deviations observed in the collected particulate mass between the liquid collector and the filter can be attributed to the variation in activation and droplet growth efficiency within the TCALC, potential insignificant particle or droplet losses during condensational growth, and particulate sample loss during sample transfer and gravimetric measurement. Despite these variations, the strong agreement between the two collection techniques showed the successful use of the TCALC for direct aerosol collection in a liquid.

The TCALC was evaluated for an inlet aerosol flow temperature of approximately 22 °C; therefore, higher ambient temperatures would necessitate cooling the aerosol stream prior to mixing with the vapor. Moreover, we selected to evaluate TCALC using NaCl aerosol, which is commonly used for the calibration of water-based condensation devices (Cheng, 2011), and crystalline silica aerosol due to its relevance to our current research needs concerning workplace aerosol measurements. However, further investigation is needed to assess the impact of aerosol chemical composition and extended operation times (up to at least 8 h) on collection efficiency.

The TCALC can eliminate the need for sample redeposition on filters suitable for specific analytical measurements, such as the quantification of redeposited crystalline silica on silver filters using XRD (NIOSH Method 7500; NIOSH, 2003a). Additionally, it can be used as an alternative to direct filter collection when analyte needs to be in a liquid suspension, as in NIOSH Method 7300 for metal detection using ICP-AES (NIOSH, 2003b). Integrating particle collection using the TCALC with spectroscopy analysis methods such as ICP-AES, would be beneficial for evaluating the limits of detection (LODs) achievable with the liquid collector compared to other aerosol sampling and analytical techniques.

4. Conclusions

The design and evaluation of a new, compact, high-throughput, Turbulent-mixing Condensation Aerosol-in-Liquid Concentrator (TCALC) for direct aerosol collection as liquid suspension was described. The TCALC unit measures approximately 12 × 16 × 18 cm. The collector can effectively operate at an aerosol sampling flowrate ranging from 8 to 10 L min^{-1}, using personal sampling pumps. Higher sampling flowrates required higher vapor temperatures to achieve near–complete activation. Nanoparticles with an initial aerodynamic diameter ≥25 nm were grown to droplets with an optical diameter >1400 nm, with an efficiency ≥80%. Active cooling of the growth tube, where the droplet growth mainly occurs, significantly optimized the efficacy of the collector, particularly at higher sampling flowrates. The measured droplet growth efficiency was >80% for aerosol RH values of ≥9% at 8 L min^{-1}, ≥80% for aerosol $RH \geq 30\%$ at 9 L min^{-1}, and >85% for aerosol $RH \geq 40\%$ at 10 L min^{-1}. We measured complete aerosol collection for number concentrations of ≤3 × 10^5 cm^{-3}. Negligible particulate mass losses were observed when comparing the TCALC's collection performance with that of conventional filter collection. The TCALC eliminates the need for sample preparation and filter digestion during chemical analysis, offering the potential for substantially improved sensitivity of off-line trace analysis of collected liquid samples. The TCALC shows promise as a high-thoughput collector allowing access to several laboratory analytical and microscopy methods, without requiring time- and labor-intensive sample preparation methods.

Supplementary Material

Refer to Web version on PubMed Central for supplementary material.

Acknowledgments

The authors would like to thank Derek Stinson for his contribution to building the prototype described in this work and for assisting with the experimental study.

Funding

This research was supported by a NIOSH intramural NORA grant (CAN 9390G1Y).

Data availability

Data will be made available on request.

References

Agarwal JK, & Sem GJ (1980). Continuous flow, single-particle-counting condensation nucleus counter. Journal of Aerosol Science, 11(4), 343–357. 10.1016/0021-8502(80)90042-7

Barhate PG, Le TC, Shukla KK, Lin ZY, Hsieh TH, Nguyen TTN, Li Z, Pui DYH, & Tsai CJ (2022). Effect of aerosol sampling conditions on PM2.5 sampling accuracy. Journal of Aerosol Science, 162. 10.1016/j.jaerosci.2022.105968

Bricard J, Delattre P, Madelaine G, & Pourprix M (1976). Detection of ultra-fine particles by means of a continuous flux condensation nuclei counter. In Liu BYH (Ed.), Fine particles (pp. 565–580). New York: Academic Press.

Cheng Y (2011). Condensation particle counters. In Kulkarni P, Baron PA, & Willeke K (Eds.), Aerosol measurement: Principles, techniques, and ApplicationsAerosol measurement: Principles, techniques, and applications (pp. 381–392). Wiley. 10.1002/9781118001684.ch17.

Chien CH, Theodore A, Wu CY, Hsu YM, & Birky B (2016). Upon correlating diameters measured by optical particle counters and aerodynamic particle sizers. Journal of Aerosol Science, 101, 77–85. 10.1016/j.jaerosci.2016.05.011

Daher N, Ning Z, Cho AK, Shafer M, Schauer JJ, & Sioutas C (2011). Comparison of the chemical and oxidative characteristics of particulate matter (PM) collected by different methods: Filters, impactors, and BioSamplers. Aerosol Science & Technology, 45(11), 1294–1304. 10.1080/02786826.2011.590554

Eiguren Fernandez A, Lewis GS, & Hering SV (2014). Design and laboratory evaluation of a sequential spot sampler for time-resolved measurement of airborne particle composition. Aerosol Science & Technology, 48(6), 655–663. 10.1080/02786826.2014.911409 [PubMed: 25045199]

Gao D, Fang T, Verma V, Zeng L, & Weber RJ (2017). A method for measuring total aerosol oxidative potential (OP) with the dithiothreitol (DTT) assay and comparisons between an urban and roadside site of water-soluble and total OP. Atmospheric Measurement Techniques, 10(8), 2821–2835. 10.5194/amt-10-2821-2017

Hering SV, Lewis GS, Spielman SR, & Eiguren-Fernandez A (2019). A MAGIC concept for self-sustained, water-based, ultrafine particle counting. Aerosol Science & Technology, 53(1), 63–72. 10.1080/02786826.2018.1538549

Hering SV, Stolzenburg MR, Quant FR, Oberreit DR, & Keady PB (2005). A laminar-flow, water-based condensation particle counter (WCPC). Aerosol Science & Technology, 39(7), 659–672. 10.1080/02786820500182123

Hinds WC, & Kraske G (1986). Performance of PMS model LAS-X optical particle counter. Journal of Aerosol Science, 17(1), 67–72. 10.1016/0021-8502(86)90007-8

Hinds WC, & Zhu Y (2022). Aerosol technology: Properties, behavior, and measurement of airborne particles (3rd ed.). Wiley.

Jang J, Bhardwaj J, & Jang J (2022). Efficient measurement of airborne viable viruses using the growth-based virus aerosol concentrator with high flow velocities. Journal of Hazardous Materials, 434, Article 128873. 10.1016/j.jhazmat.2022.128873 [PubMed: 35427967]

Khlystov A (1995). The steam-jet aerosol collector. Atmospheric Environment, 29(17), 2229–2234. 10.1016/1352-2310(95)00180-7

Kidwell CB, & Ondov JM (2001). Development and evaluation of a prototype system for collecting sub-hourly ambient aerosol for chemical analysis. Aerosol Science & Technology, 35(1), 596–601. 10.1080/02786820118049

Kim CS, Okuyama K, & de la Mora JF (2003). Performance evaluation of an improved particle size magnifier (PSM) for single nanoparticle detection. Aerosol Science & Technology, 37(10), 791–803. 10.1080/02786820300913

Kim CS, Okuyama K, & Shimada M (2002). Performance of a mixing-type CNC for nanoparticles at low-pressure conditions. Journal of Aerosol Science, 33(10), 1389–1404. 10.1016/S0021-8502(02)00092-7

Kousaka Y, Niida T, Okuyama K, & Tanaka H (1982). Development of a mixing type condensation nucleus counter. Journal of Aerosol Science, 13(3), 231–240. 10.1016/0021-8502(82)90064-7

Lewis GS, & Hering SV (2013). Minimizing concentration effects in water-based, laminar-flow condensation particle counters. Aerosol Science & Technology, 47 (6), 645–654. 10.1080/02786826.2013.779629 [PubMed: 24436507]

Liu CN, Lin SF, Awasthi A, Tsai CJ, Wu YC, & Chen CF (2014). Sampling and conditioning artifacts of PM2.5 in filter-based samplers. Atmospheric Environment, 85, 48–53. 10.1016/j.atmosenv.2013.11.075

Mavliev R (2002). Turbulent mixing condensation nucleus counter. Atmospheric Research, 62(3–4), 303–314. 10.1016/S0169-8095(02)00016-9

Nannu Shankar S, Vass WB, Lednicky JA, Logan T, Messcher RL, Eiguren-Fernandez A, Amanatidis S, Sabo-Attwood T, & Wu C-Y (2024). The BioCascade-VIVAS system for collection and

delivery of virus-laden size-fractionated airborne particles. Journal of Aerosol Science, 175, Article 106263. 10.1016/j.jaerosci.2023.106263 [PubMed: 38680161]

NIOSH. (2003a). SILICA, CRYSTALLINE, by XRD (filter redeposition): Method 7500. In NIOSH manual of analytical methods (NMAM). Edition: Fourth. https://www.cdc.gov/niosh/docs/2003-154/pdfs/7500.pdf.

NIOSH. (2003b). ELEMENTS by ICP (Nitric/Perchloric acid ashing): Method 7300. In NIOSH manual of analytical methods (NMAM). Edition: Fourth. https://www.cdc.gov/niosh/docs/2003-154/pdfs/7300.pdf.

Okuyama K, Kousaka Y, & Motouchi T (1984). Condensational growth of ultrafine aerosol particles in a new particle size magnifier. Aerosol Science & Technology, 3 (4), 353–366. 10.1080/02786828408959024

Okuyama K, Kousaka Y, Warren DR, Flagan RC, & Seinfeld JH (1987). Homogeneous nucleation by continuous mixing of high temperature vapor with Room temperature gas. Aerosol Science & Technology, 6(1), 15–27. 10.1080/02786828708959116

Orsini DA, Ma Y, Sullivan A, Sierau B, Baumann K, & Weber RJ (2003). Refinements to the particle-into-liquid sampler (PILS) for ground and airborne measurements of water soluble aerosol composition. Atmospheric Environment, 37(9–10), 1243–1259. 10.1016/S1352-2310(02)01015-4

Parsons C, & Mavliev R (2001). Design and characterization of a new, water-based, high sample-flow condensation nucleus counter. Aerosol Science & Technology, 34(4), 309–320. 10.1080/02786820117366

Raynor PC, Leith D, Lee KW, & Mukund R (2011). Sampling and analysis using filters. In Kulkarni P, Baron PA, & Willeke K (Eds.), Aerosol measurement (pp. 107–128). Wiley. 10.1002/9781118001684.ch7.

Ryan PH, Son SY, Wolfe C, Lockey J, Brokamp C, & LeMasters G (2015). A field application of a personal sensor for ultrafine particle exposure in children. The Science of the Total Environment, 508, 366–373. 10.1016/j.scitotenv.2014.11.061 [PubMed: 25497676]

Sgro L, & Fernández de la Mora J (2004). A simple turbulent mixing CNC for charged particle detection down to 1.2 nm. Aerosol Science & Technology, 38(1), 1–11. 10.1080/02786820490247560

Sinclair D, & Hoopes GS (1975). A continuous flow condensation nucleus counter. Journal of Aerosol Science, 6(1), 1–7. 10.1016/0021-8502(75)90036-1.

Sorooshian A, Brechtel FJ, Ma Y, Weber RJ, Corless A, Flagan RC, & Seinfeld JH (2006). Modeling and characterization of a particle-into-liquid sampler (PILS). Aerosol Science & Technology, 40(6), 396–409. 10.1080/02786820600632282

Wang D, Jiang J, Deng J, Li Y, & Hao J (2020). A sampler for collecting fine particles into liquid suspensions. Aerosol and Air Quality Research, 20(3), 654–662. 10.4209/aaqr.2019.12.0616

Wang J, McNeill VF, Collins DR, & Flagan RC (2002). Fast mixing condensation nucleus counter: Application to rapid scanning differential mobility analyzer measurements. Aerosol Science & Technology, 36(6), 678–689. 10.1080/02786820290038366

Wang D, Pakbin P, Saffari A, Shafer MM, Schauer JJ, & Sioutas C (2013). Development and evaluation of a high-volume aerosol-into-liquid collector for fine and ultrafine particulate matter. Aerosol Science & Technology, 47(11), 1226–1238. 10.1080/02786826.2013.830693

Weber RJ, Orsini D, Daun Y, Lee Y-N, Klotz PJ, & Brechtel F (2001). A particle-into-liquid collector for rapid measurement of aerosol bulk chemical composition. Aerosol Science & Technology, 35(3), 718–727. 10.1080/02786820152546761

Wubulihairen M, Sabrina Jiang, Y., & Ning Z (2015). Prototype development and laboratory evaluation of an aerosol to hydrosol sampler. Aerosol and Air Quality Research, 15(3), 776–785. 10.4209/aaqr.2014.08.0175

Zervaki O, Dionysiou DD, & Kulkarni P (2024). Compact, high-flow, water-based, turbulent-mixing, condensation aerosol concentrator for collection of spot samples. Aerosol Science & Technology, 58(8), 889–901. 10.1080/02786826.2024.2361050 [PubMed: 39376592]

Zervaki O, Stump B, Keady P, Dionysiou DD, & Kulkarni P (2023). NanoSpot TM collector for aerosol sample collection for direct microscopy and spectroscopy analysis. Aerosol Science & Technology, 57(4), 342–354. 10.1080/02786826.2023.2167648 [PubMed: 37284690]

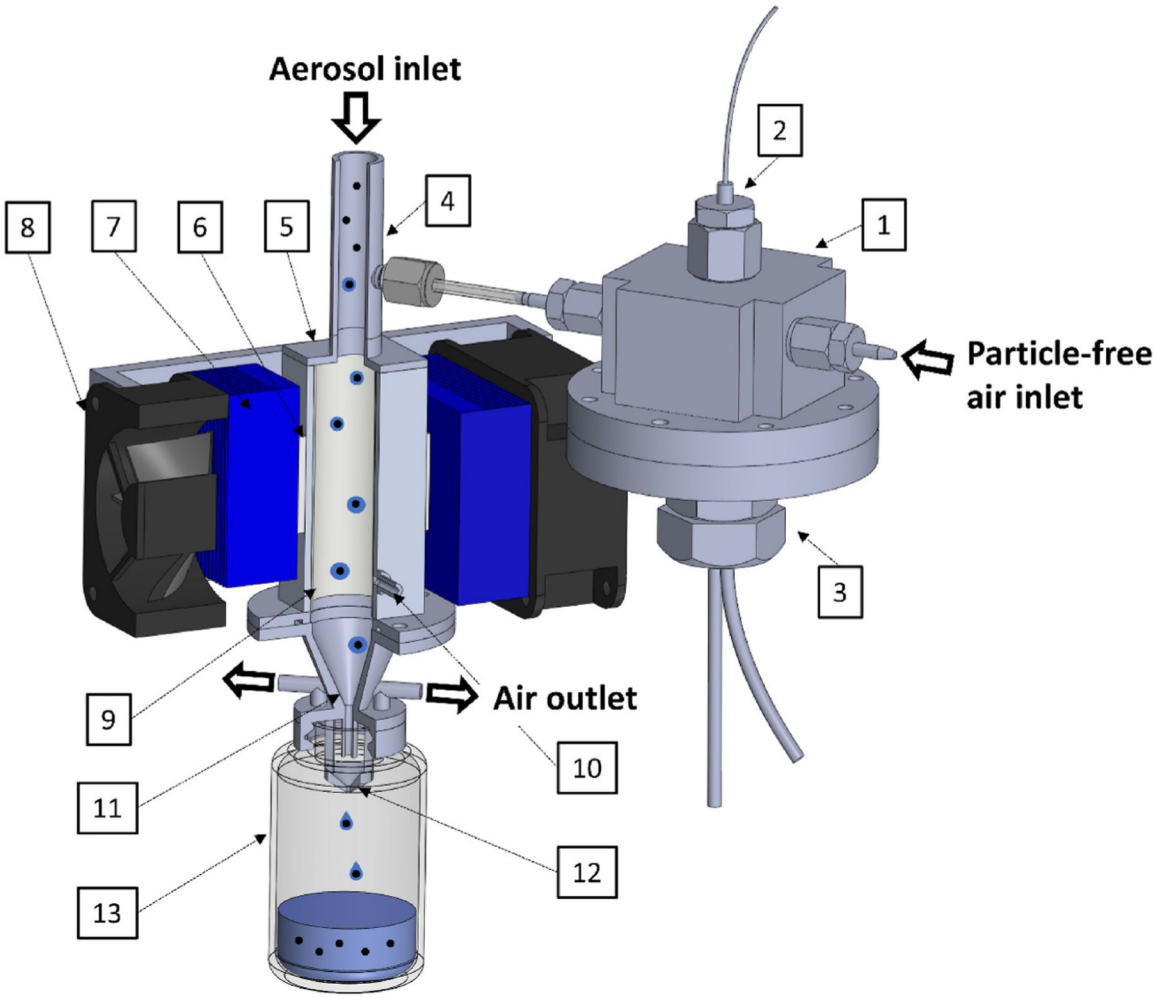

Fig. 1.

3D view of the TCALC apparatus. (1) Saturator, (2) Resistance Temperature Detector (RTD), (3) Cartridge heater, (4) Mixing region, (5) Droplet growth region, (6) Thermoelectric cooler (TEC), (7) Heatsink, (8) Fan, (9) Durapore® PVDF membrane, (10) Outlet of condensed water, (11) Focusing nozzle, (12) Droplet impactor, (13) Collection vial.

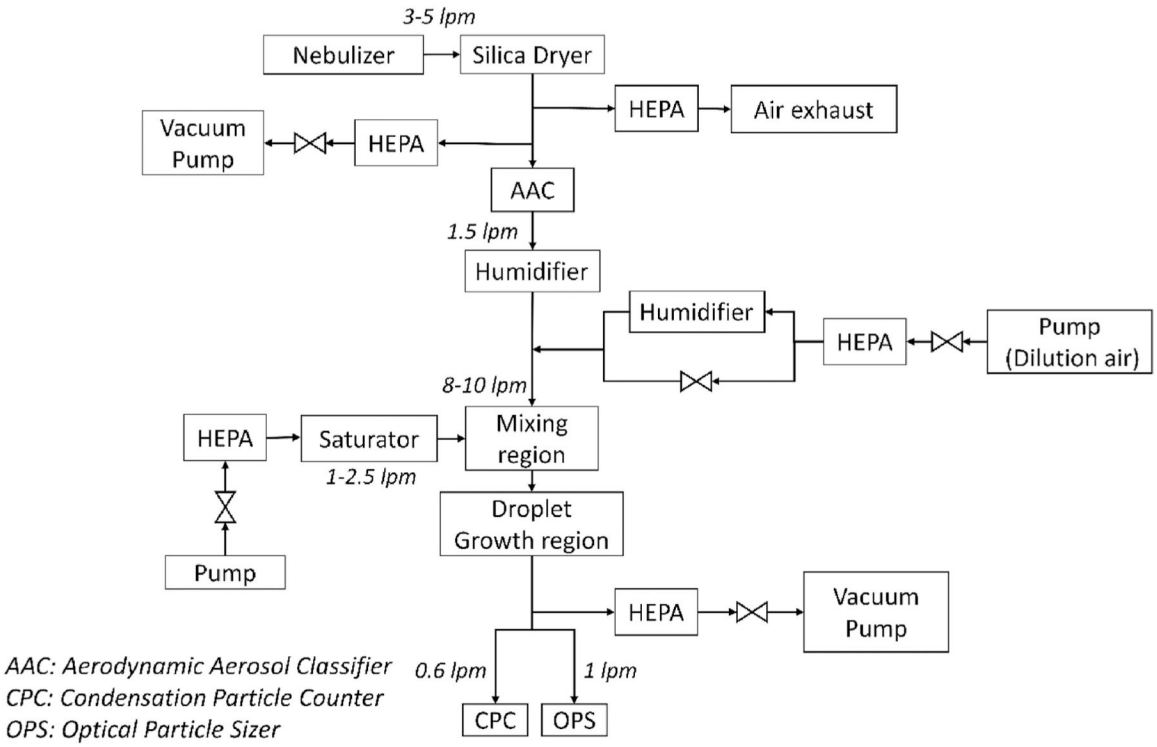

Fig. 2.

Experimental setup used for measurement of droplet growth efficiency obtained through the mixing and droplet growth region of the TCALC.

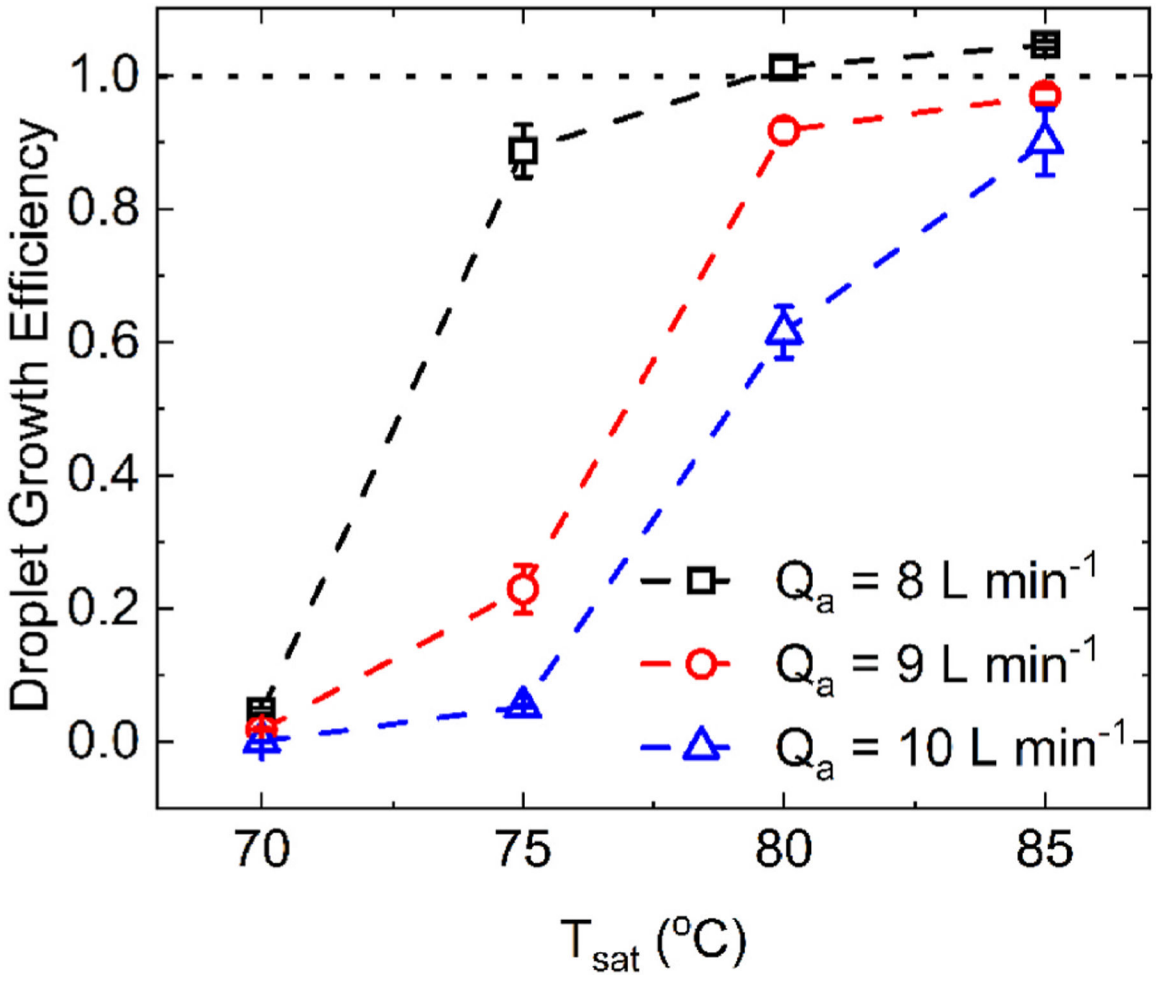

Fig. 3.

Droplet growth efficiency (d_d > 1.4 μm) measured as a function of the saturator temperature (T_{sat}, °C) for an aerosol flowrate of 8, 9 and 10 L min^{-1}. 100-nm-diameter NaCl particles were used (T_a = 23.6 – 24.9 °C, RH = 45.8 – 51.5%, T_{gt} = 0 °C). The error bars indicate the standard deviation of three repeat measurements.

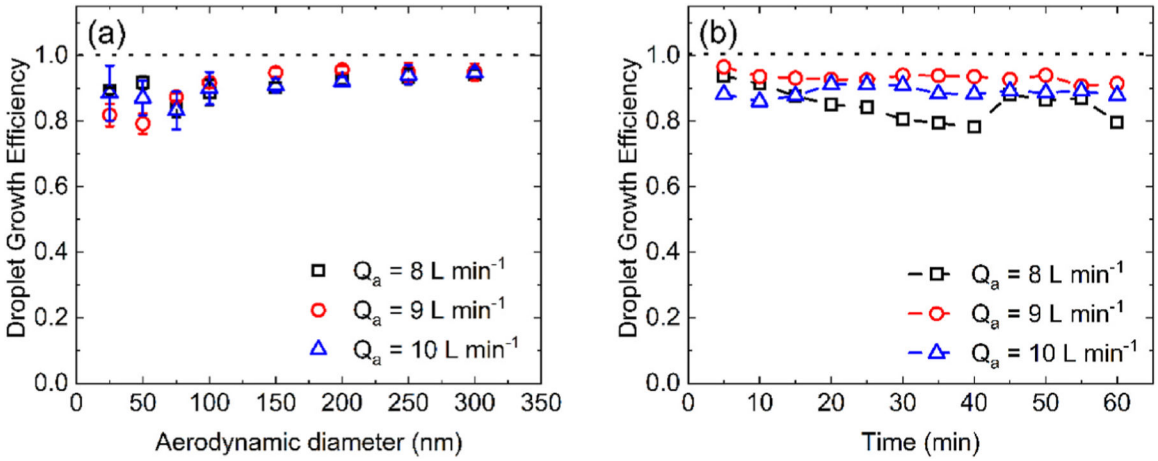

Fig. 4.

Droplet growth efficiency ($d_d > 1.4$ μm) measured as a function of (a) the seed particle aerodynamic diameter (d_p, nm) and (b) the operation time (min), for a fixed aerosol flowrate of 8 L min^{-1} ($T_{sat} = 75$ °C), 9 L min^{-1} ($T_{sat} = 80$ °C) and 10 L min^{-1} ($T_{sat} = 85$ °C). NaCl particles were used. 100-nm-diameter particles were used for the evaluation of the impact of the operation time ($T_a = 22.5 – 25.3$ °C, $RH = 46.6 – 56\%$). The error bars in (a) indicate the standard deviation of three repeat measurements.

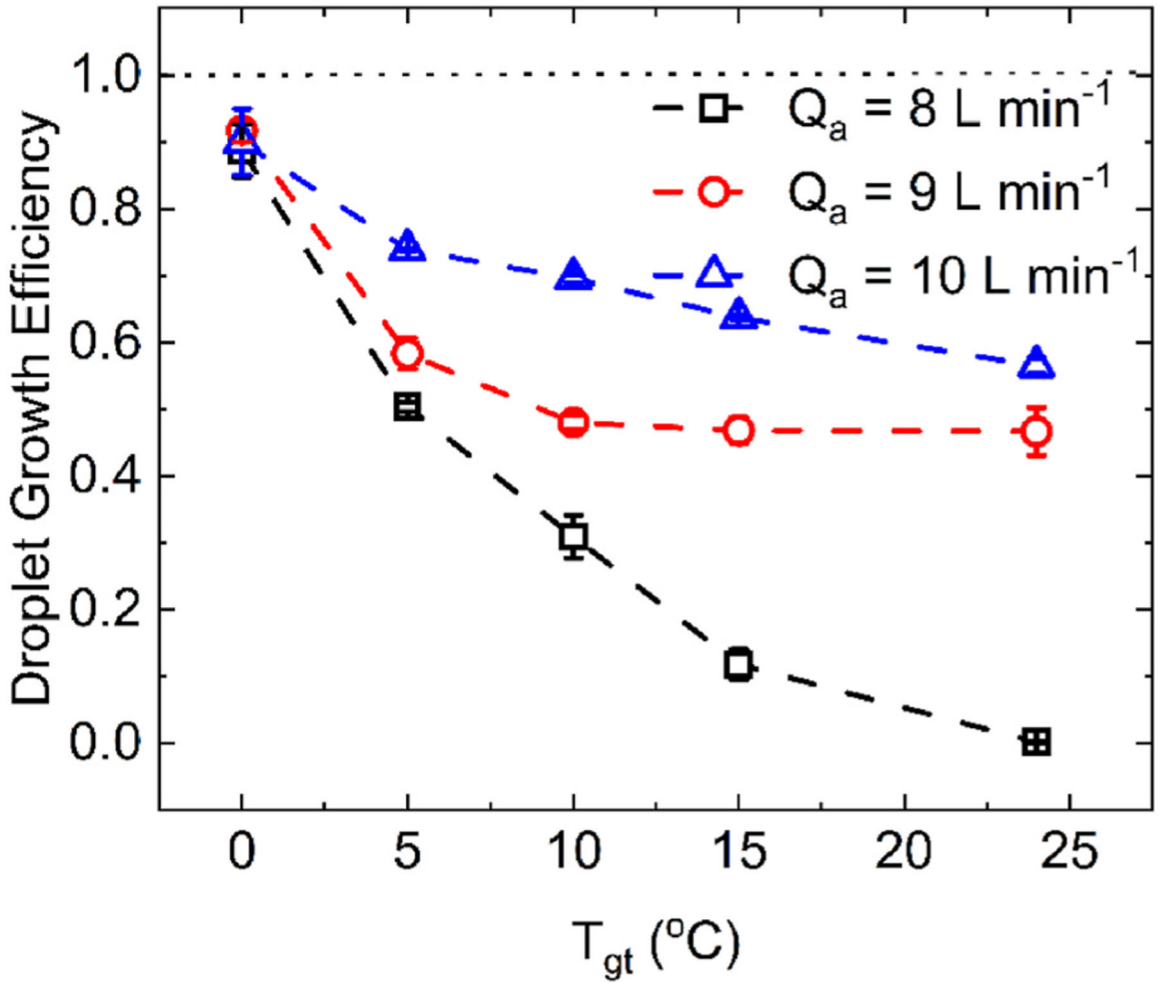

Fig. 5.

Droplet growth efficiency ($d_d > 1.4$ μm) measured as a function of the growth tube temperature (T_{gt}, °C) for an aerosol flowrate of 8 L min^{-1} (T_{sat} = 75 °C), 9 L min^{-1} (T_{sat} = 80 °C) and 10 L min^{-1} (T_{sat} = 85 °C). 100-nm-diameter NaCl particles were used (T_a = 23.7 – 24.9 °C, RH = 46.5 – 52.2%). The error bars indicate the standard deviation of three repeat measurements.

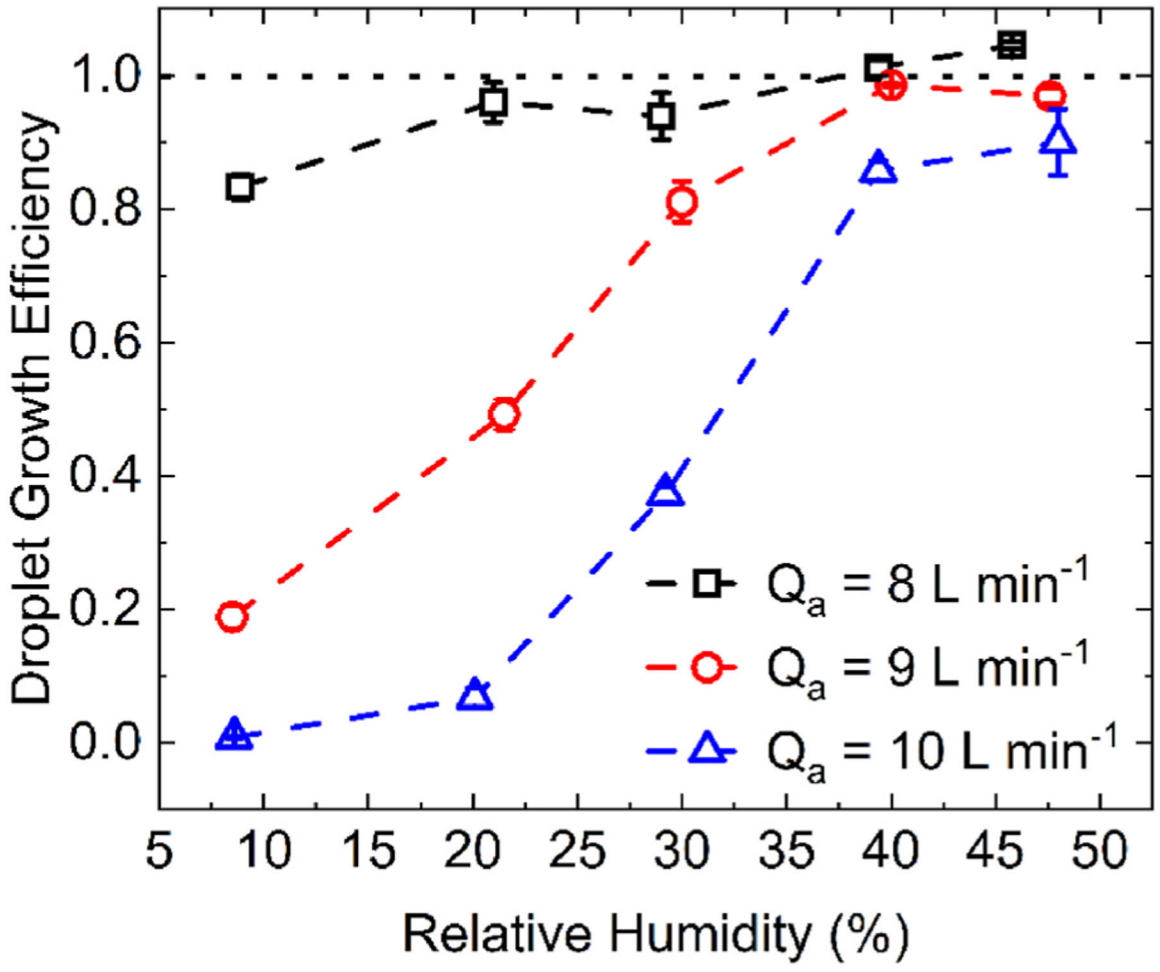

Fig. 6.

Droplet growth efficiency ($d_d > 1.4$ μm) measured as a function of the aerosol inlet relative humidity (%) for an aerosol flowrate of 8, 9 and 10 L min^{-1}. 100-nm-diameter NaCl particles were used (T_a = 23.6 – 25.4 °C and T_{sat} = 85 °C). The error bars indicate the standard deviation of three repeat measurements.

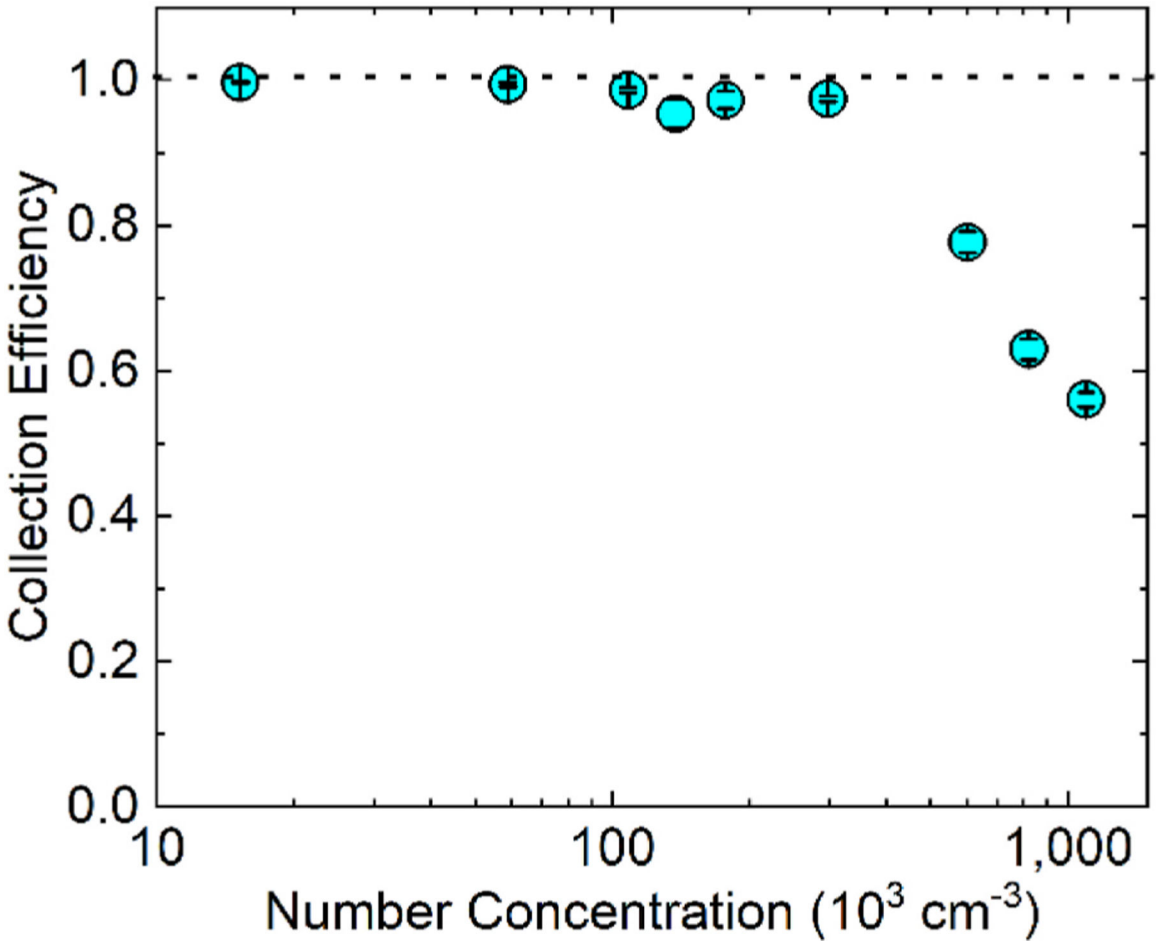

Fig. 7.

Collection efficiency of crystalline silica particles as a function of the number concentration (RH = 40.2 – 57.4%, T_a = 22.3 – 22.8 °C, Q_a = 10 L min^{-1}, T_{sat} = 85 °C, T_{gt} = 0 °C). The error bars, too small to be clearly visible, indicate the standard deviation of three repeat measurements.

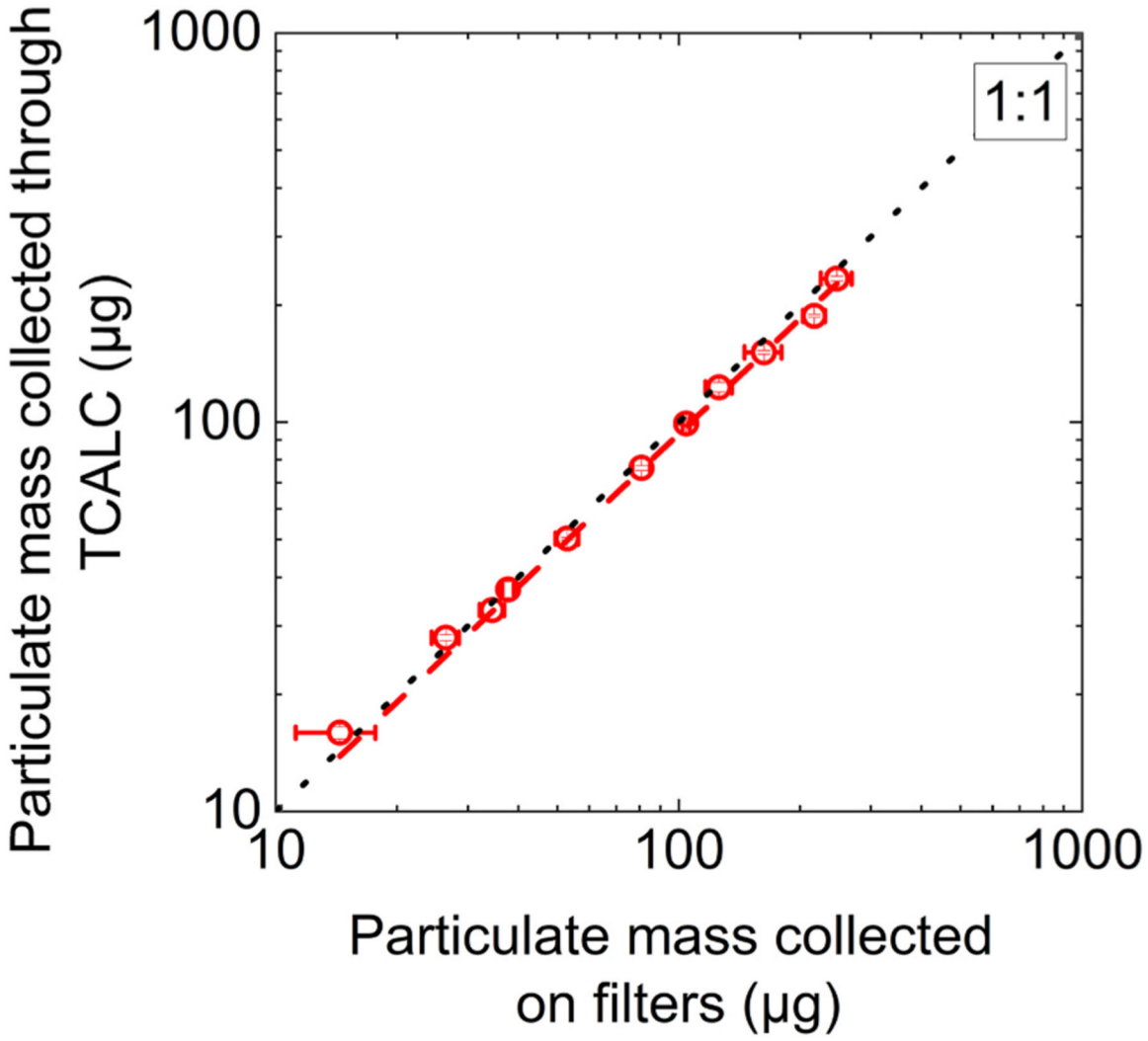

Fig. 8.

Comparison of crystalline silica particulate mass (μg) collected through the TCALC and reference 37-mm-diameter polycarbonate filters. The error bars represent the standard deviation of three gravimetric repeat measurements. The dashed line represents the linear fit of the experimental data.